Available on CMS information server

CMS CR -2010/183

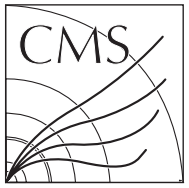

The Compact Muon Solenoid Experiment

Conference Report

Mailing address: CMS CERN, CH-1211 GENEVA 23, Switzerland

20 October 2010 (v2, 24 October 2010)

CMS Tracking, Alignment and Physics Performances results

Andrea Venturi for the CMS Collaboration

Abstract

The CMS all-silicon tracker was aligned using more than three millions cosmic rays particles. The positions of the modules were determined with respect to cosmic ray trajectories to a precision of 3-4 microns RMS in the barrel and 3-14 microns RMS in the endcap in the most sensitive coordinate. The trajectories of charged particles produced in the LHC collisions were reconstructed and their momenta were measured in the 3.8T solenoidal magnetic field. Reconstructed tracks are used to determine the position of the primary interaction vertex in the event and to monitor the position of the colliding beams. The tracks have been used further to reconstruct the hadronic decays of several mesons, including K0s, Lambda, and phi. The performance of track reconstruction has been measured in the data and is compared to the expectation from simulation.

Presented at *Vertex 2010: Vertex 2010*

PROCEEDINGS OF SCIENCE

CMS Alignment Tracking and Physics Performance Results

Andrea Venturi[*†]
INFN Sezione di Pisa, Pisa, Italy
E-mail: andrea.venturi@cern.ch

The CMS all-silicon tracker was aligned using more than three millions cosmic rays particles. The positions of the modules were determined with respect to cosmic ray trajectories to a precision of $3-4\,\mu$m RMS in the barrel and $3-14\,\mu$m RMS in the endcap in the most sensitive coordinate. The trajectories of charged particles produced in the LHC collisions were reconstructed and their momenta were measured in the 3.8 T solenoidal magnetic field. Reconstructed tracks are used to determine the position of the primary interaction vertex in the event and to monitor the position of the colliding beams. The tracks have been used further to reconstruct the hadronic decays of several mesons, including K^0_s, Λ^0, and ϕ. The performance of track reconstruction has been measured in the data and is compared to the expectation from simulation

19th International Workshop on Vertex Detectors
June 6 -11 2010
Loch Lomond, Scotland, UK

[*]Speaker.
[†]On behalf of CMS Collaboration

1. The CMS Tracking Detector

The CMS detector is one of the four detectors installed at the Large Hadron Collider (LHC) at CERN [1]. It has been designed to record and reconstruct pp collisions at $\sqrt{s} = 14$ TeV with an istantaneous luminosity of about $10^{34}\,\mathrm{cm}^{-2}\mathrm{s}^{-1}$. The key element of the CMS detector is the superconducting solenoid, 13 m long with a diameter of 6 m, operated to produce a magnetic field of 3.8 T within its volume. Inside the solenoid, from outside to inside, there is a brass-scintillator hadron calorimeter, a cristal electromagnetic calorimeter and an all-silicon tracking detector for the reconstruction of the trajectories of the charged particles. Outside the solenoid, embedded in the iron yoke, there are the gaseous detectors to identify the muons and reconstruct their trajectories and momenta together with the inner tracker.
The inner tracker is composed of a pixel silicon detector with three barrel layers at radii between 4.4 cm and 10.2 cm and two endcap disks at each end, and a silicon strip tracker with 10 barrel detection layers extending to a radius of 1.1 m and 3+9 disks on each side of the barrel to extend the overall tracker acceptance up to pseudorapidity $|\eta| < 2.5$. The total active surface is about 200 m^2, the largest silicon tracker ever built. The pixel size is $100 \times 150\,\mu\mathrm{m}^2$ for a total of 66M channels while the strip tracker is equipped with sensors with different pitches, from 80 to 180 μm, leading to about 9.6 M channels. In the strip tracker 4 layers in the barrel and 3 rings in the endcaps are equipped with paired sensors with a 100 mrad relative stereo angle among the strips to provide accurate 3-dimensional hits. This granularity was chosen to balance the need for a low occupancy, which is expected to be a few percent at the nominal LHC luminosity, and the requirement to keep the the power density, the needed cooling power and the amount of material at the minimum. The basic performance expected for the tracking detector is a transverse momentum resolution of about $1-2\%$ for muons of $p_t \sim 100\,\mathrm{GeV}$, an impact parameter resolution of about $10-20\,\mu$m for tracks with $p_t \sim 10-20\,\mathrm{GeV}$ and the ability to reconstruct tracks in hadronic jets with an efficiency of about $85-90\%$ and a fake rate not exceeding a few percent.

2. First LHC Collisions and Cosmic Runs

In December 2009 LHC produced the first pp collisions at $\sqrt{s} = 900$ and 2360 GeV. Due to the relatively low LHC luminosity ($< 10^{27}\,\mathrm{cm}^{-2}\mathrm{s}^{-1}$) the CMS readout was triggered by the beam scintillator counters placed close to the beam line to collect minimum-bias collision events. About 260,000 events produced in this period were selected and used to study, for the first time, the performance of the CMS silicon tracker with pp collisions. Since March 2010 LHC has run at $\sqrt{s} = 7\,\mathrm{TeV}$, the new top energy for a particle accelerator. In the first weeks of this run the luminosity conditions still allowed the use of the minimum-bias trigger. The results described in this report are based on the data collected in 2009 or at the beginning of the 2010 run. Details of the commissioning and of the operation of the pixel and the strip tracking detectors are in the contributions to the proceedings of this conference [2, 3]
Prior to the LHC pp collision runs, CMS performed two long runs with a cosmic ray muon trigger in 2008 and 2009 and one in 2010 before the LHC run, during which about 10 millions muon tracks were recorder, reconstructed and studies with the tracking detector. This large amount of data allowed to syncronize the tracking detector to the CMS trigger, to tune the configuration of the

readout chain, to exercise the local reconstruction of the hits and the global reconstruction of the tracks [4, 5] performing, among others, measurements of the single hit efficiency and resolution, of the tracking efficiency and of the track parameter resolutions. Finally these data have been used to perform the alignment of the tracker sensors, as described below, and to monitor its stability over a long period and in different operating conditions.

3. Tracker Alignment

The good hit position resolution of the silicon tracker, ranging from about 10 to 30 μm, requires a knowledge of the position of the 15148 (strip) + 1440 (pixel) sensors with a comparable or better accuracy. The results of the optical surveys performed at each step of the tracker construction are a very useful starting point but do not provide the required accuracy and cannot correct the time dependent changes of the geometry which occurred after the tracker installation. Therefore alignment algorithms based on the track reconstruction are used for the final determination of the sensor positions and orientations. The core of the track-based alignment is the minimization of the χ^2 of the hit-track residuals with respect to the parameters describing the sensor positions. Two algorithms have been developed and are used in CMS [6]. The *Millipede II* algorithm performs a global minimization of the χ^2 including also the track parameters which are optmized together with the sensor position parameters. To achieve that, the dependence on the track parameters are linearized and an *ad hoc* track model is used with respect to the standard reconstruction. The sensor alignment parameters are determined by solving a matrix equation of the order of 10^5 elements. The *Hit and Impact Points* (HIP) algorithm performs a local minimization of the χ^2 with respect the position of each sensor; the parameters of the track used to compute the residuals are fixed and determined by excluding the sensor under study from the track fit. The correlation among the alignment parameters of different modules and the track parameters are taken into account, effectively, by iterating the procedure several times and using the alignment parameters of the previous iteration to re-reconstruct the tracks used in the χ^2 computation. The HIP algorithm allows to include the results of the optical surveys as constraints in the χ^2 minimization. Finally the two alignment algorithms are applied sequentially, using the alignment parameters determined by the first as starting point for the second, and the procedure is applied firstly on large scale substructures and finally at the sensor level.

The alignment parameters have been determined three times, with the cosmic muon tracks in 2008 and 2009 and, finally, in 2010 with about 1.5 million of cosmic tracks (p>4 GeV) and about 1.7 million collision tracks (p>3 GeV). The complementarity of the cosmic and collision track samples allowed to achieve a good accuracy both in the barrel and in the endcaps of the tracker. In figure 1 are shown the distributions of the median of the residuals (DMR) of each sensor with at least 200 hits on tracks. The RMS of these distributions are a useful figure to quantify the accuracy of the alignment: they are below 6 μm in the barrel and 10 μm in the endcaps. In figure 2 the distribution of the track normalized χ^2 obtained with the aligned geometry is shown and compared with the predictions from simulations with no misalignment or with a realistic misalignment (STARTUP).

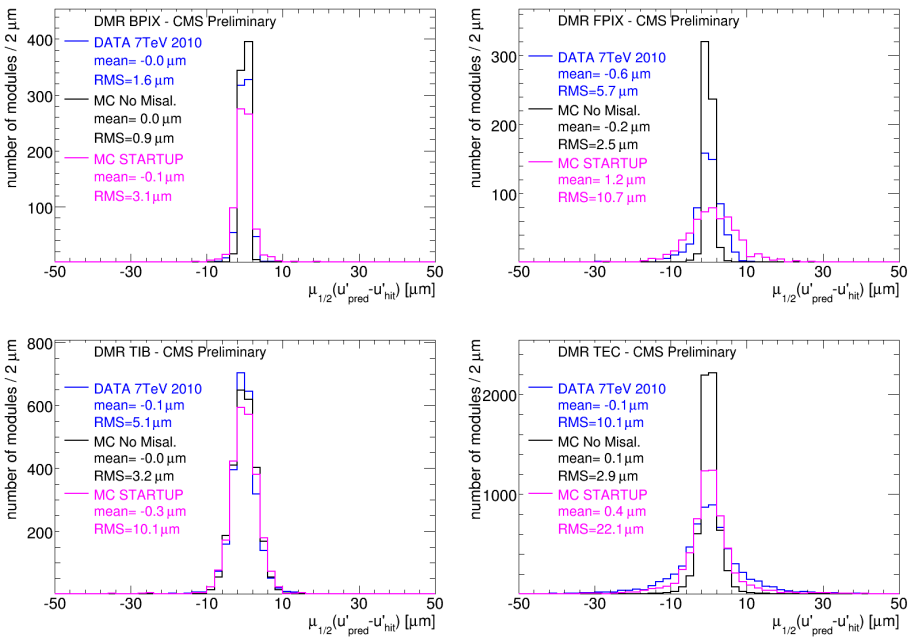

Figure 1: Distributions of the hit residual medians for sensors with more than 200 hits in barrel pixel (top left), endcap pixel (top right) strip inner barrel (bottom left) and strip endcaps (bottom right). Results from real data are compared to simulations with no or realistic misalignment.

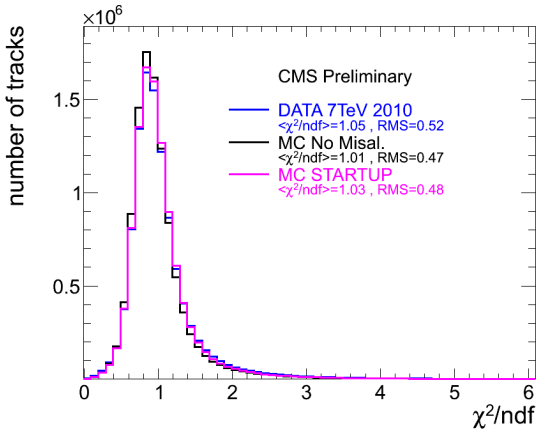

Figure 2: Distribution of the normalized χ^2 of the reconstructed tracks in $\sqrt{s}$ =7 TeV collisions compared to simulations with no or realistic misalignment.

4. The Tracker Physics Performance

The first LHC collision data recorded by CMS represent an important step for the commissioning of the tracking detector and of the track reconstruction. Due to the low luminosity the events collected in 2009 and in the first weeks of 2010 did not probe extremely challenging region of the phase space in term of track transverse momentum, track multiplicity and track density. Nevertheless they have been extremely useful to assess the basic features of the performance of the tracker and of the reconstruction among which: the syncronization of the tracker readout the the LHC beam, the measurement of the actual hit occupancy, its comparison with the simulation, and the performance of the track reconstruction pattern recognition with the actual occupancy. The full operation, readout and reconstruction chain worked smoothly and as expected and the system proved to be robust also with respect to unexpected high multiplicity beam background events [7]. In addition the tracking detector data has been very useful as a first feedback for the tuning of the simulations of non-perturbative QCD processes.
In general all the measured observables have been compared to the simulation tuned to reproduce the realistic detector conditions in term of disconnected channels (98.3% and 98.1% active channels in pixel and strip tracker respectively) and alignment accuracy. The results are shown in the following sections and more details can be found in Refs. [8, 9].

4.1 Track Reconstruction

In CMS the tracks are reconstructed in four steps. The first is the seeding step when hit triplets or pairs (plus the beam spot constraint) from the pixel tracker or the inner layers of the strip tracker are selected and used as track candidate. The second is the pattern recognition step when track candidates are propagated using a Kalman filter technique to find new compatible hits and the track parameters are updated. In this step track candidates are rejected if not enough hits are found. The third step is the final track fit when the track parameters are estimated combining all the associated hits. At this stage hits can be rejected if they look incompatible to the fitted track. Finally the tracks are given a quality flag based on a set of cuts sensitive to fake tracks and based on track normalized χ^2, track compatibility with interaction region, track length and number of missed hits. The tracks which pass the tightest selection are classified as *high purity* tracks [9] while those which do not fulfill the loosest set of cuts are discarded. All the above steps are iterated six times: at each iteration the hits associated to the high purity tracks are discarded and the seeding and the pattern recognition steps are performed using the remaining hits. This allows, at each iteration, to have looser cuts at the seeding step and at the final track selection step, thanks to the reduced combinatorial background. In addition a dedicated track and primary vertex reconstruction based only on pixel tracker hits is performed to provide a set of primary vertices which can be used for the full track reconstruction and also in the High Level Trigger algorithms which are run online, thanks to the speed of this simple reconstruction.
Inclusive distributions of the parameters of the tracks reconstructed in the minimum-bias collision events collected at $\sqrt{s} = 900\,\text{GeV}$, 2.36 TeV and 7 TeV have been compared to the simulation predictions. In figure 3 the distributions obtained at 7 TeV are compared to the predictions obtained with the PYTHIA 8 [10] generator with the default tuning and a full GEANT-based simulation of the CMS detector. In these distributions only high purity tracks with a longitudinal impact pa-

rameter significance smaller than 10, to remove the contributions of the looping low momentum tracks, an estimated transverse momentum error better than 5%, to remove short tracks, and with $p_t > 0.5\,\text{GeV}$, to be less sensitive to the disagreement of the simulation tuning to the low-p_t region of the phase space, are shown. The good observed agreement reassures that the track reconstruction and in particular the pattern recognition works as expected also with the actual hit occupancy and there is no stricking evidence of inefficiencies or anomalous fake rates. In particular the distributions of the track pseudo-rapidity and azimuthal angle and of the number of hits per track prove that the simulation is able to reproduce tiny details thanks to a detailed description of the tracker geometry and of the dead channels.

4.2 Invariant mass distributions

A further step in the commissioning of the tracking detector and of the track reconstruction with the first collisions has been the reconstruction of the invariant masses of tracks from unstable particle and resonance decays. The invariant mass distributions with the presence of narrow peaks provide references which can be used to compare momentum calibration and resolution between real data and simulation. With the data collected in 2009 and 2010 only low mass particle and resonance decays have been produced with a sizeable statistics and in a (transverse) momentum range of the order of a few GeV or less. Therefore the phase space region which can be sensitive to misalignment or to details of the single hit resolution has not been explored, yet. Nevertheless the comparison with the simulation provides a valuable tool to check the simulation of the multiple scattering and of the energy loss due to the detector material, which affect mostly the low momentum particles. Furthermore the relative contribution between the signal region and the combinatorial background is used to check the simulation of the background itself and to provide feedback for the tuning of the simulation of the production yield of these particles.
$K^0_s \to \pi^+\pi^-$ and $\Lambda^0 \to p\pi^-$ decay (V^0) invariant mass distributions have been produced with pairs of opposite charge tracks: they are required to be of good quality and to have a transverse impact parameter not compatible with the interaction region within 0.5σ. These pairs of tracks are fitted to a common vertex and if the fit is successful and with a good χ^2, the pair is kept if the significance of the transverse distance of the vertex from the interaction region is larger than 15. In the case of the Λ^0 decay candidate, the particle with the largest momentum is given the proton mass. In figure 4 the invariant mass distributions of the K^0_s and Λ^0 decay candidates fitted with a double Gaussian function are shown. The resolutions obtained from the average of the two Gaussian resolutions are 8.0 MeV and 3.0 MeV for K^0_s and Λ^0, respectively, in good agreement with the MC predictions (7.6 MeV and 3.0 MeV).
The V^0s selected in this way are combined either with another track incompatible with the interaction region to reconstruct decay cascades (Ξ^-, Ω^-) or with tracks from the interaction region to look for strongly decaying strange resonances ($K^*(892)$, $\Sigma^{\pm}(1385)$, $\Xi^0(1530)$). In figure 5 the $\Lambda^0\pi^-$ invariant mass distribution, with a clear $\Xi^- \to \Lambda^0\pi^-$ peak, and the $K^0_s\pi^-$ invariant mass distribution with a clear $K^*(892)$ signal are shown. In both cases the V^0 tracks are refitted with the proper V^0 mass constraint.
The data collected at the beginning of 2010 run, about 10 million of minimum bias events, have been used to search for D meson decays. For example the $D^* \to D^0\pi \to K\pi\pi$ decay chain has

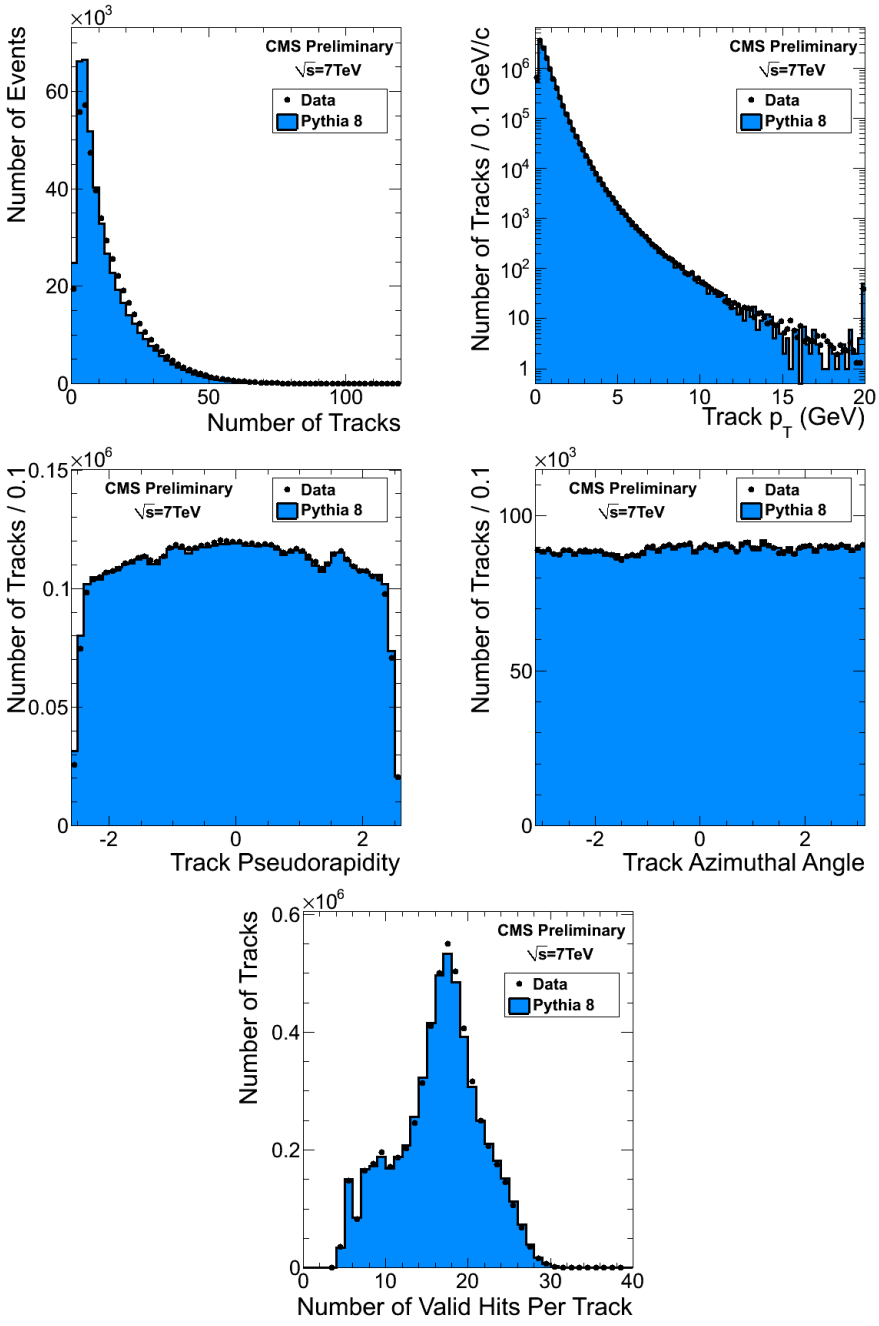

Figure 3: Distributions of: track multiplicity (top left), transverse momentum (top right), pseudorapidity (center left), azimuthal angle (center right) and the number of hits on track (bottom), for *high purity* tracks with $p_t > 0.5\,\text{GeV}$, $\sigma(p_t)/p_t < 5\%$ and $d_z/\sigma(d_z) < 10$ in 7 TeV collisions events selected with a minimum bias trigger, compared to the PYTHIA 8 predictions.

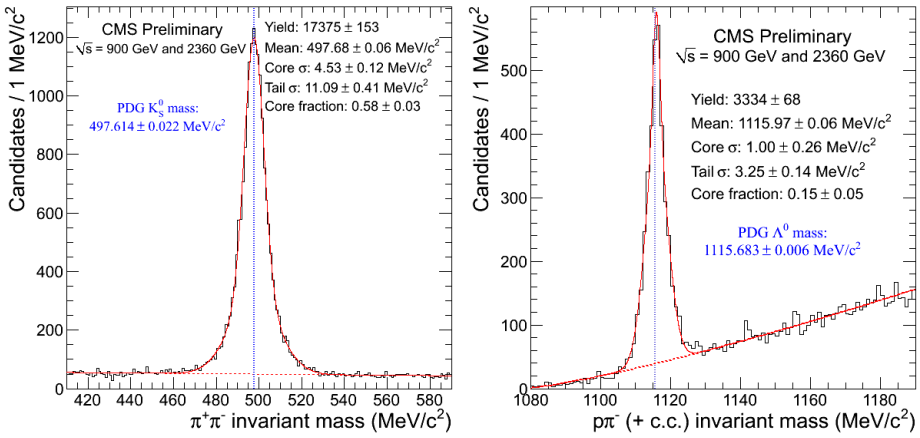

Figure 4: $K^0_s \to \pi^+\pi^-$ (left) and $\Lambda^0 \to p\pi^-$ (right) candidate invariant mass distributions obtained with 900 GeV collision events.

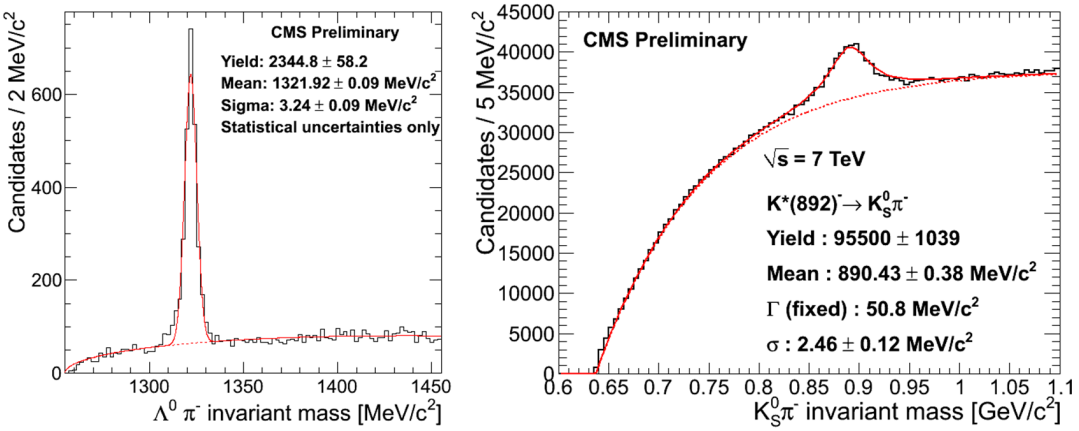

Figure 5: $\Lambda^0\pi^-$ (right) and $K^0_s\pi^-$ (left) invariant mass distributions obtained with 7 TeV collision events.

been studied by pairing opposite charge tracks with $p_t > 600\,\text{MeV}$ and which form a good vertex; if the invariant mass is close to the D^0 mass by less than 25 MeV, a third track with $p_t > 250\,\text{MeV}$ is combined to form the D^* candidate. In figure 6 the distribution of the invariant mass difference between $K\pi\pi$ and $K\pi$ systems, when the $K\pi$ mass is close to the D^0 mass less than 25 MeV, and the distribution of the $K\pi$ invariant mass, when the mass difference is compatible to the nominal value better than 1.2 MeV, are shown. The parameters of the fitted functions are in agreement with the simulation.

Presently, thanks to the large amount of collected data after the conference, the invariant mass distributions are used also for quantitative estimate and calibration of the tracking performance. The K^0_s mass distributions, together with that of the $J/\psi \to \mu\mu$ decays, are used to study the momentum scale calibration and resolution [11]. The tracking efficiency [12] has been studied by comparing the ratio of observed $D^* \to D^0\pi \to (K\pi\pi\pi)\pi$ to $D^* \to D^0\pi \to (K\pi)\pi$ decays and applying the

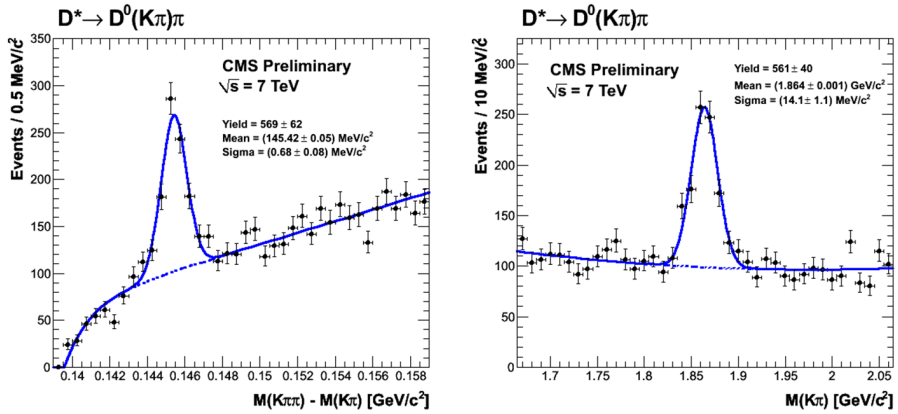

Figure 6: Distribution of the invariant mass M($K\pi\pi$)-M($K\pi$) difference (left) and of the $K\pi$ invariant mass (right) obtained with 7 TeV collision events.

tag-and-probe algorithm to the $J/\psi \to \mu\mu$ decays where the tag is a fully reconstructed muon and the probe is a muon reconstructed only in the CMS muon detectors and its reconstruction in the inner tracking detector is probed.

Finally the invariant mass distribution of the $\phi \to KK$ has been studied. For this analysis the ability to measure the ionization energy loss, dE/dx, of the reconstructed tracks, thanks to the analog read-out of the silicon tracker, has been used and tested. In figure 7 (left) the measured dE/dx and the momentum of the reconstructed tracks is shown: the analog signal used to compute the armonic estimator has been calibrated for each sensor using minimum ionizing particles. In the low p region the contributions of K and protons are clearly visible. Using the relation, $\frac{dE}{dx} = K\frac{m^2}{p^2} + C$ and determining the parameters K and C from proton-enriched region, it is possible to obtain an estimate of the particle mass for each track. In figure 7 (right) the distribution of the estimated mass is shown for tracks with $dE/dx > 4.15\,\mathrm{MeV/cm}$ with clear peaks from K and protons and the evidence that the deuterons are not properly simulated. The main use of this estimator is the search for heavy stable charged particles which cross the tracker volume and release more energy than a minimum ionizing particles.

In the $\phi \to KK$ analysis, to reduce the combinatorial background, tracks with $p < 1\,\mathrm{GeV}$ are kept only if the mass estimated from the dE/dx measurement is compatible to the K mass within 200 MeV. In figure 8 the KK invariant mass distribution is shown and compared to the distribution obtained by selecting, instead, only tracks with $p < 1\,GeV$ and a dE/dx measurement incompatible with the K hypothesis. The latter does not show any hint of ϕ decays.

4.3 Primary Vertex and Luminous Region Reconstruction

The reconstruction of the collision primary vertices and of the three-dimensional profile of the luminous region where the LHC beams collide, is one of the important measurement performed with the CMS silicon tracker. LHC beams, at 7 TeV, have a width of a few tens of microns (a few hundreds of microns in the 2009 run at 900 and 2360 GeV) and a bunch length of a few cm. Therefore the reconstruction of the interaction primary vertices in each event is crucial to determine the

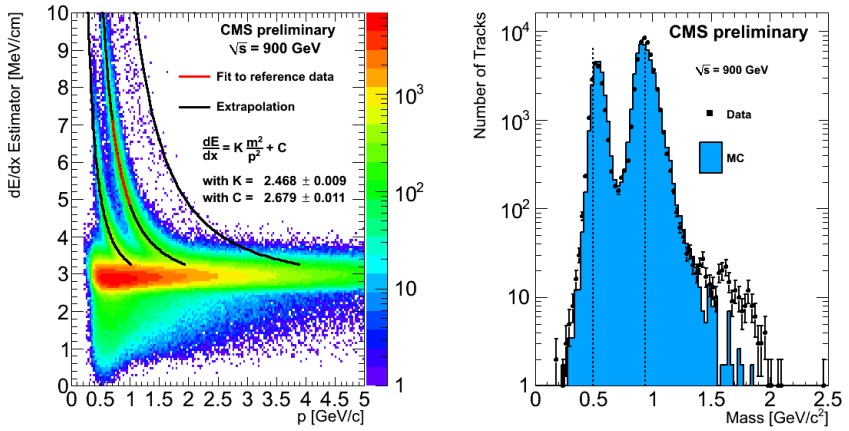

Figure 7: Distribution of the dE/dx estimator vs the track momentum (left) and distribution and estimated particle mass (right) obtained with 900 GeV collision events.

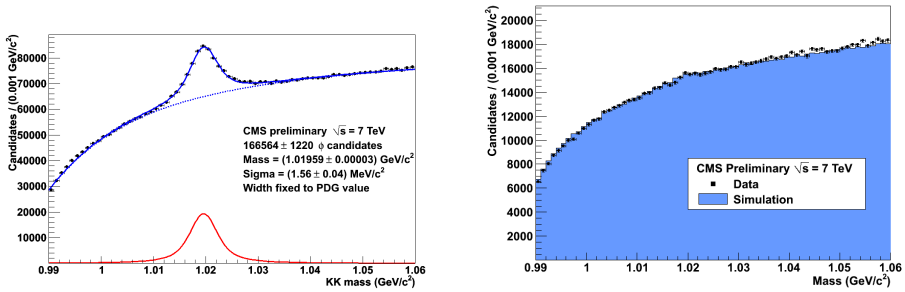

Figure 8: *KK* invariant mass distributions obtained with the signal-enriched selection (left) and with the anti-K-hypothesis selection (right) using the 7 TeV collision events.

longitudinal (z) position of the interaction within the bunch profile, while the determination of the luminous region over many events allows a more accurate determination of the beam transverse position. A precise determination of these parameters is needed for the track reconstruction, when a constraint to the interaction point is required, and for analyses which need to identify tracks from displaced vertices like the tagging of b-quark jets. Furthermore the determination of the interaction primary vertex longitudinal positions and their multiplicity is a key element to deal with the pile-up of pp interactions in each bunch crossing: an efficient vertex reconstruction and an accurate z position determination allow to discriminate among tracks produced by the hard interaction and those produced by the additional soft interactions.

With the data collected in 2009 the resolution of the measured primary vertex position has been estimated by splitting the tracks in each event in two samples and reconstructing a vertex from each sample. The RMS of the distributions of the differences of the vertex positions along the three axis for each pair, divided by $\sqrt{2}$, are interpreted as the resolution. This measurement has been performed as a function of the number of tracks, as shown in figure 9, and also as a function of the average p_t of the tracks. In both cases the expected behaviour has been observed with a better res-

olution for high multiplicity vertices and for vertices with tracks with higher p_t due to the reduced effect of the multiple scattering in the tracker material. The agreement with the simulation is good, certifing a good simulation of the multiple scattering, which is the main contribution to the resolution for such soft events. Also the event-by-event comparison of the vertex position differences with the estimated uncertainties show a good reliability of the estimated uncertainty.

The determination of the luminous region over many events is performed both using a likelihood

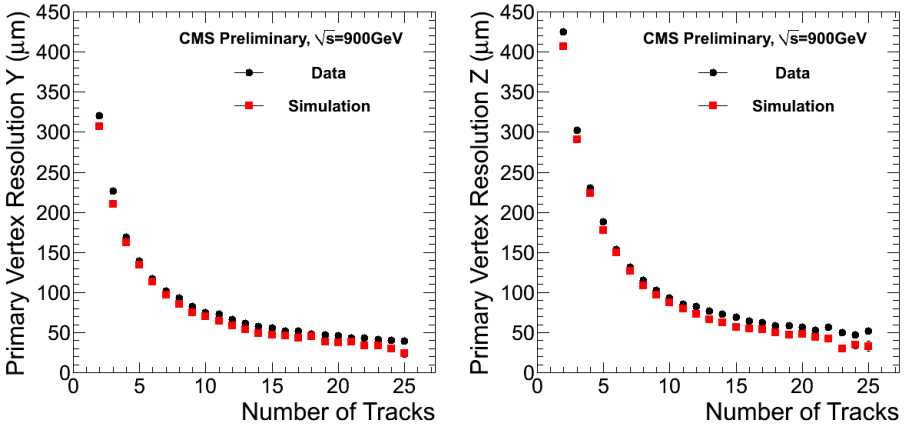

Figure 9: Primary vertex position resolution along the y (left) and the z (right) axes as a function of the track multiplicity measured with 900 GeV collision events.

fit to the three-dimensional distribution of the primary vertex positions and by exploiting the correlation between the track transverse impact parameter and the track azimuthal angle: if the beam line is displaced from the reference point used to compute the impact parameter, the correlation is sinusoidal, as shown in figure 10 (left), with an amplitude and a phase which depends on the actual position of the beam line. In figure 10 (right) the luminous region positions measured with the two methods are compared. The fit to the primary vertex distribution allows also the measurement of the beam width. These parameters are determined every 23 s and averaged over many intervals to improve the accuracy if no sizeable differences are observed. More recent results obtained with a larger statistics can be found in Ref. [13].

4.4 Preliminary b-tagging performance studies

The silicon tracker and in particular the pixel detector, plays an important rôle in the b-quark jet tagging algorithms. The main observables which rely on the track reconstruction are the track impact parameter significance and the properties of the secondary vertices [14]. The data collected in 2009 and the first data collected in 2010 ($\sim 1\,\mathrm{nb}^{-1}$) allowed to compare some basic distributions obtained with the real data with the simulation predictions. In figure 11 the distribution of the 3D impact parameter significance for tracks in jets with $p_t > 40\,\mathrm{GeV}$ and the track multiplicity of the secondary vertices in jets with $p_t > 10\,\mathrm{GeV}$ show a good agreement with the simulation. Results obtained with a larger statistics collected in 2010 are described in Ref. [15].

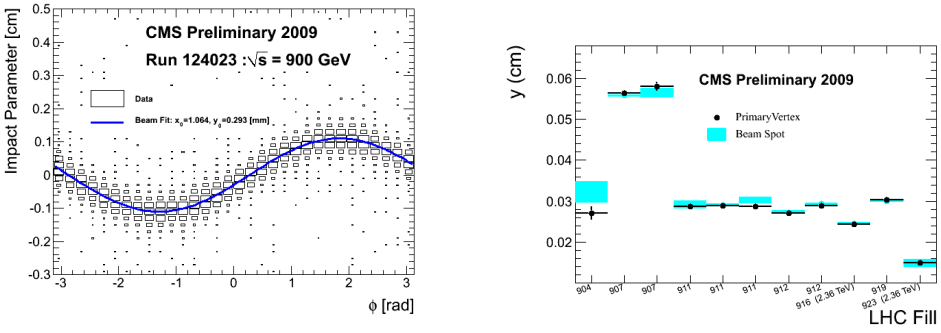

Figure 10: Correlation between the track impact parameter and the azimuthal angle (left) and beam line transverse position along the y axis (right) measured in different LHC fills during the 2009 run.

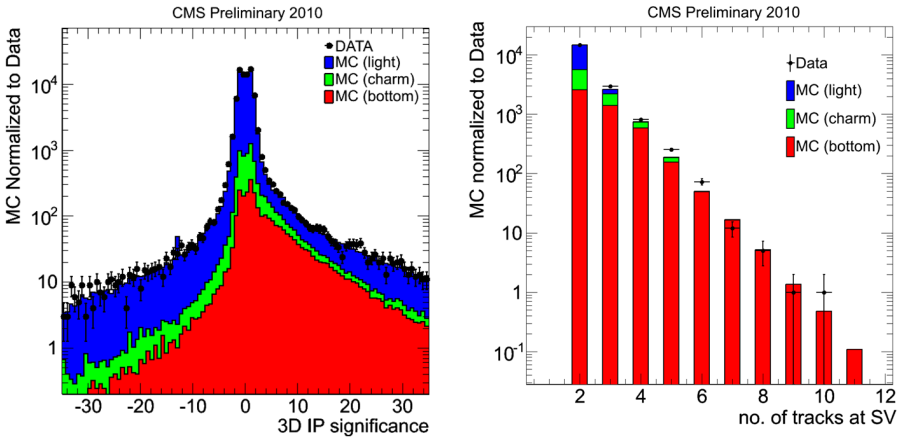

Figure 11: Three-dimensional impact parameter significance distribution for tracks in jets with $p_t > 40\,\text{GeV}$ (left) and track multiplicity in reconstructed secondary vertices in jets with $p_t > 10\,\text{GeV}$ (right) in events from 7 TeV collisions.

4.5 Tracker Material Studies

The amount of material that a particle has to cross in the silicon tracker volume is far from being negligible: about 0.4 radiation lengths for tracks with pseudorapidity $\eta = 0$ and about 1.7 X_0 at $\eta = 1.5$. This cause a sizeable amount of photon conversions into e^+e^- pairs, bremsstrahlung emission by electrons and nuclear interactions of the charged hadrons with the tracker material (about 5% of the pions). Therefore the simulation of the tracker material and of the interactions has to be compared carefully with the real data and, if needed, fine tuned. With the data collected in 2009, dominated by low-p_t tracks and photons from π^0 decays, two techniques based on the reconstruction of the photon conversions and of the nuclear interactions have been tested. The photon conversions are reconstructed by pairing tracks with opposite charge, small opening angle at the point of closest approach between the trajectories projected in the transverse plane, and

small longitudinal separation at this point. The selected pairs are fitted with a constraint to a common vertex and imposing that the tracks are parallel at the vertex. If the fit converges the pair is selected as conversion candidate. Nuclear interaction vertices are reconstructed by fitting to a common vertex set of tracks pre-selected recursively by pairing tracks with small relative distance of closest approach. Finally V^0 and conversion candidates are removed from the nuclear interaction candidates. The low stastistics and low transverse momentum of the 2009 data samples allow to probe with some sensitivity only the tracker region corresponding to the first two layers of the pixel tracker: only tracks with hits in at least two pixel layers can be reconstructed efficiently down to $p_t \sim 100\,\text{MeV}$. In figure 12 the distribution of the positions in the transverse plane of the reconstructed nuclear interaction vertices in the barrel region is shown. The profile of the beam pipe is clearly visible as well as the pixel detector inner surface and the structures of the first pixel tracker layer.
The results obtained with the larger statistics collected in 2010 and with additional dedicated track reconstruction iterative steps to improve the efficiency, are described in Ref. [16] where a more quantitative estimate of the tracker material simulation quality is provided.

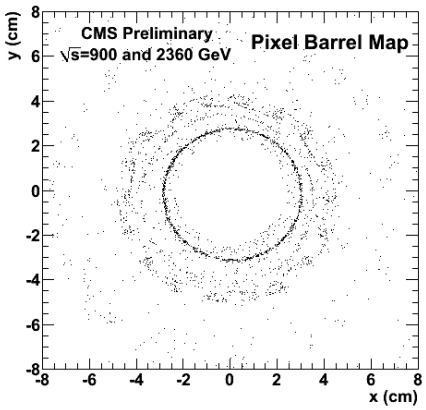

Figure 12: Distribution of the nuclear interaction vertices in the region of the pixel tracker reconstructed in the events from 900 GeV collisions.

5. Conclusions

The data collected with the first LHC collisions in 2009 and in the first part of the 2010 run have shown that the performance of the CMS tracker and of the track reconstruction is excellent and the simulation is in good agreement. The increasing amount of data collected during the 2010 run is used to perform more quantitative studies about the tracking efficiency, the momentum calibration and resolution and the tracker material description and to improve the alignment. At the same time CMS has been publishing its first physics results among which those related to the study of the properties of the reconstructed charged tracks are: the measurement of the transverse momentum and pseudorapidity distributions of the charged hadrons, the measurement of the Bose-Einstein correlations and the study of the particle angular correlations [17].

References

[1] CMS Collaboration, *The CMS Experiment at the CERN LHC*, JINST **0803** (2008) S08004. doi:10.1088/1748-0221/3/08/S08004

[2] E. Butz, CMS Collaboration, *CMS Silicon strips operations and performance*, in these proceedings.

[3] K. Ecklund, CMS Collaboration, *CMS pixel operations and performance*, in these proceedings.

[4] CMS Collaboration, *Commissioning and Performance of the CMS Pixel Tracker with Cosmic Ray Muons*, JINST **5** (2010) T03007. doi:10.1088/1748-0221/5/03/T03007

[5] CMS Collaboration, *Commissioning and Performance of the CMS Silicon Strip Tracker with Cosmic Ray Muons*, JINST **5** (2010) T03008. doi:10.1088/1748-0221/5/03/T03008

[6] CMS Collaboration, *Alignment of the CMS Silicon Tracker during Commissioning with Cosmic Rays* , JINST **5** (2010) T03009. doi:10.1088/1748-0221/5/03/T03009

[7] H. Snoek, CMS Collaboration, *Beam background effects in the CMS pixel detector*, in these proceedings.

[8] CMS Collaboration, *CMS Tracking Performance Results from Early LHC Operation*, CERN-PH-EP-2010-019 (2010), to be published in Eur. J. Phys. C. arXiv:1007.1988

[9] CMS Collaboration, *Tracking and Vertexing Results from First Collisions*, CMS Physics Analysis Summary, CMS-TRK-10-001 (2010).

[10] T. Sjöstrand, S. Mrenna and P. Skands, *A Brief Introduction to PYTHIA 8.1*, Comput. Phys. Commun. **178** (2008) 852.

[11] CMS Collaboration, *Measurement of Momentum Scale and Resolution using Low-mass Resonances and Cosmic-Ray Muons*, CMS Physics Analysis Summary, CMS-TRK-10-004 (2010).

[12] CMS Collaboration, *Measurement of Tracking Efficiency*, CMS Physics Analysis Summary, CMS-TRK-10-002 (2010).

[13] CMS Collaboration, *Tracking and Primary Vertex Results in First 7 TeV Collisions*, CMS Physics Analysis Summary, CMS-TRK-10-005 (2010).

[14] CMS Collaboration, *Algorithms for b Jet identification in CMS*, CMS Physics Analysis Summary, CMS-BTV-09-001 (2009).

[15] CMS Collaboration, *Commissioning of b-jet identification with pp collisions at* $\sqrt{s} = 7$ *TeV* , CMS Physics Analysis Summary, CMS-BTV-10-001 (2010).

[16] CMS Collaboration, *Studies of Tracker Material*, CMS Physics Analysis Summary, CMS-TRK-10-003 (2010).

[17] CMS Collaboration, *Transverse momentum and pseudorapidity distributions of charged hadrons in pp collisions at* $\sqrt{s} = 0.9$ *and 2.36 TeV*, J. High Energy Phys. **2** (2010) 041. doi:10.1007/JHEP02(2010)041
CMS Collaboration, *First Measurement of Bose-Einstein Correlations in proton-proton Collisions at* $\sqrt{s}$ *=0.9 and 2.36 TeV at the LHC*, Phys. Rev. Lett. **105** (2010) 032001. doi:10.1103/PhysRevLett.105.032001
CMS Collaboration, *Transverse-momentum and pseudorapidity distributions of charged hadrons in pp collisions at* $\sqrt{s} = 7$ *TeV* , Phys. Rev. Lett. : **105** (2010) 022002. doi:10.1103/PhysRevLett.105.022002
CMS Collaboration, *Observation of Long-Range, Near-Side Angular Correlations in Proton-Proton Collisions at the LHC*, J. High Energy Phys. **09** (2010) 091. doi:10.1007/JHEP09(2010)091